CrossMark

ORIGINAL PAPER

Novel mutations confirm that *COL11A2* is responsible for autosomal recessive non-syndromic hearing loss DFNB53

Imen Chakchouk · M'hamed Grati · Guney Bademci · Mariem Bensaid · Qi Ma · Amine Chakroun · Joseph Foster II · Denise Yan · Duygu Duman · Oscar Diaz-Horta · Abdelmonem Ghorbel · Rahul Mittal · Amjad Farooq · Mustafa Tekin · Saber Masmoudi · Xue Zhong Liu

Abstract Hearing loss (HL) is a major public health issue. It is clinically and genetically heterogeneous. The identification of the causal mutation is important for early diagnosis, clinical follow-up, and genetic counseling. HL due to mutations in *COL11A2*, encoding collagen type XI alpha-2, can be non-syndromic autosomal-dominant or autosomal-recessive, and also syndromic as in Otospondylomegaepiphyseal Dysplasia, Stickler syndrome type III, and Weissenbacher–Zweymuller syndrome. However, thus far only one mutation co-segregating with autosomal recessive non-syndromic hearing loss (ARNSHL) in a single family has been reported. In this study, whole exome sequencing of two consanguineous families with ARNSHL from Tunisia and Turkey revealed two novel causative *COL11A2* mutations, c.109G > T (p.Ala37Ser) and c.2662C > A (p.Pro888Thr). The variants identified co-segregated with deafness in both families. All homozygous individuals in those families had early onset profound hearing loss across all frequencies without syndromic findings. The variants are predicted to be damaging the protein function. The p.Pro888Thr mutation affects a -Gly-X–Y- triplet repeat motif. The novel p.Ala37Ser is the first missense mutation located in the NC4 domain of the COL11A2 protein. Structural model suggests that this mutation will likely obliterate, or at least partially compromise, the ability of NC4 domain to interact with its cognate ligands. In conclusion, we confirm that *COL11A2* mutations cause ARNSHL and broaden the mutation spectrum that may shed new light on genotype–phenotype correlation for the associated phenotypes and clinical follow-up.

Keywords *COL11A2* · Exome sequencing · Hearing loss · Mutation · Structural modeling

I. Chakchouk · M. Bensaid · S. Masmoudi (✉)
Laboratoire Procédés de Criblage Moléculaire et Cellulaire, Centre de Biotechnologie de Sfax, Université de Sfax, Route sidimansour Km 6, BP '1177', 3018 Sfax, Tunisia
e-mail: saber.masmoudi@cbs.rnrt.tn

M. Grati · Q. Ma · D. Yan · R. Mittal · X. Z. Liu (✉)
Department of Otolaryngology (D-48), Miller School of Medicine, University of Miami, 1666 NW 12th Avenue, Miami, FL 33136, USA
e-mail: xliu@med.Miami.edu

G. Bademci · J. Foster II · O. Diaz-Horta · M. Tekin
John P. Hussmann Institute for Human Genomics and John T. Macdonald Foundation, Department of Human Genetics, Miller school of Medicine, University of Miami, Miami, FL, USA

A. Chakroun · A. Ghorbel
Service Otorhinolaryngologie, Hôpital Universitaire Habib Bourguiba, Sfax, Tunisie

D. Duman
Division of Pediatric Genetics, Ankara University School of Medicine, Ankara, Turkey

A. Farooq
Biochemistry and Molecular Biology, Miller School of Medicine, University of Miami, Miami, FL 33136, USA

Introduction

The high prevalence/incidence of hearing impairment in man makes it the most common sensory defect. It affects one in nearly 500 newborns. The majority of the cases are of genetic origin. Identification of deafness-related mutations is of great significance in revealing the molecular pathogenesis and aiding the clinical diagnosis of this disease. Hereditary hearing loss (HL) that is not associated with other symptoms classified as non-syndromic deafness is extremely heterogeneous. Non-syndromic genetic hearing defect is inherited in autosomal recessive mode (ARNSHL) in ~77 % of the cases, autosomal dominant HL (ADNSHL) accounts for about 22 %, and the remainder ~1 % is composed of X-linked and mitochondrial forms. Over 100 ARNSHL gene loci have been localized through genome-wide linkage analysis of large pedigrees of consanguineous families, and over 60 ARNSHL genes have been so far identified (Hereditary Hearing Loss Homepage: http://hereditaryhearingloss.org/main.aspx?c=. HHH&n=86316). Most recently, the application of whole-exome sequencing (WES) for identifying deafness-causing genes in small families for whom linkage would not be informative, and in large families in which linkage intervals were too large for proceeding with candidate gene Sanger sequencing approach, has been introduced as an alternative to traditional methods (Yan et al. 2013). It has the advantage of overcoming the costly and time-consuming Sanger DNA sequencing of the tens of already known HL genes.

The tectorial membrane (TM) of the mammalian cochlea is a gelatinous sheet-like structure anchored at its inner part to the apex of the interdental cells, and lays on the top of sensory hair cells where the long rows of outer hair cell stereocilia are anchored. The structural integrity of the TM is crucial for the acquisition of its complex mechanical properties that are associated with the hearing process. TM is made of four types of collagens (II, V, IX and XI), five types of non-collagenous glycoproteins (α-tectorin, β-tectorin, otogelin, otoanchorin and otolin), glycosaminoglycans (uronic acid and keratan sulfate), and CEACAM16. Stereocilin, a protein of outer hair cells, assures the anchoring between the TM and long stereocilia. Several mutations in these proteins have been identified in human families and cause syndromic or non-syndromic HL. In particular, mutations in collagens, that are the main components of bone and cartilage, have been found to cause many types of syndromic HL (Hereditary Hearing Loss Homepage: http://hereditaryhearingloss.org/).

COL11A2 spans ~28 kb and consists of 66 exons and an alternatively spliced exon in the amino terminus (Zhidkova et al. 1995; Vuoristo et al. 1996). Mutations in *COL11A2* encoding fibrillar collagen type XI alpha2, have been found to cause syndromic HL such

as Otospondylomegaepiphyseal Dysplasia (OSMED; MIM:215150), Stickler syndrome type III (STL3; MIM: 184840) and Weissenbacher–Zweymuller syndrome (WZS; MIM: 277610), as well as non-syndromic recessive (DFNB53; MIM: 609706) and dominant (DFNA13;MIM: 601868) HL. However, only one *COL11A2* mutation leading to DFNB53 has been reported in an Iranian family (Chen et al. 2005). All affected individuals in this family had prelingual non-progressive profound HL and were homozygous for the c.1861C > A (p.Pro621Thr) mutation. Here, we present the clinical, genetic, and molecular characteristics of Tunisian and Turkish consanguineous families with non-syndromic recessive DFNB53.

Materials and methods

Patients and clinical data

This study was approved by the local Institutional Review Board at the University of Miami (USA), the Ethics Commitee of Ankara University Medical School (Turkey), and the ethical committee of the Habib Bourguiba University Hospital of Sfax (Tunisia). A signed informed consent form was obtained from each participant.

Family FT3 is a multigenerational family presenting ARNSHL. Sixteen individuals from this family agreed to participate in this study. The pedigree of the family was obtained upon interviews with parents (Fig. 1). Family FT3 members and 113 unrelated healthy individuals originated from southern Tunisia. Family 262 is a consanguineous Turkish family with two affected siblings (Fig. 2). All individuals underwent physical and otoscopic examinations. Pure-tone audiometry was performed in 10 affected and additional unaffected individuals. Air and bone conduction thresholds were measured at 0.25, 0.5, 1, 2, 4, and 8 kHz. Air-conduction pure-tone average (ACPTA) thresholds in the conversational frequencies (0.5, 1, 2, and 4 kHz) were calculated for each ear and were used to define the severity of deafness: mild (20db < ACPTA ≤ 39db), moderate (40db < ACPTA ≤ 69db), severe (70db < ACPTA ≤ 89db), and profound (≥90 db). Environmental causes such as rubella, prematurity, drug use during pregnancy, perinatal trauma, and meningitis as well as syndromic findings, especially those with facial anomalies, were excluded. Vestibular examination showed no abnormalities. The family members were also subjected to orthopedic examination; plain radiographies of the hands and the lumbar spine were performed.

Blood samples from 15 members of Tunisian family, five members of Turkish family, and 113 unrelated healthy Tunisian individuals were collected and genomic DNA was extracted following a standard phenol–chloroform method. *GJB2* mutations were found to be negative in the probands.
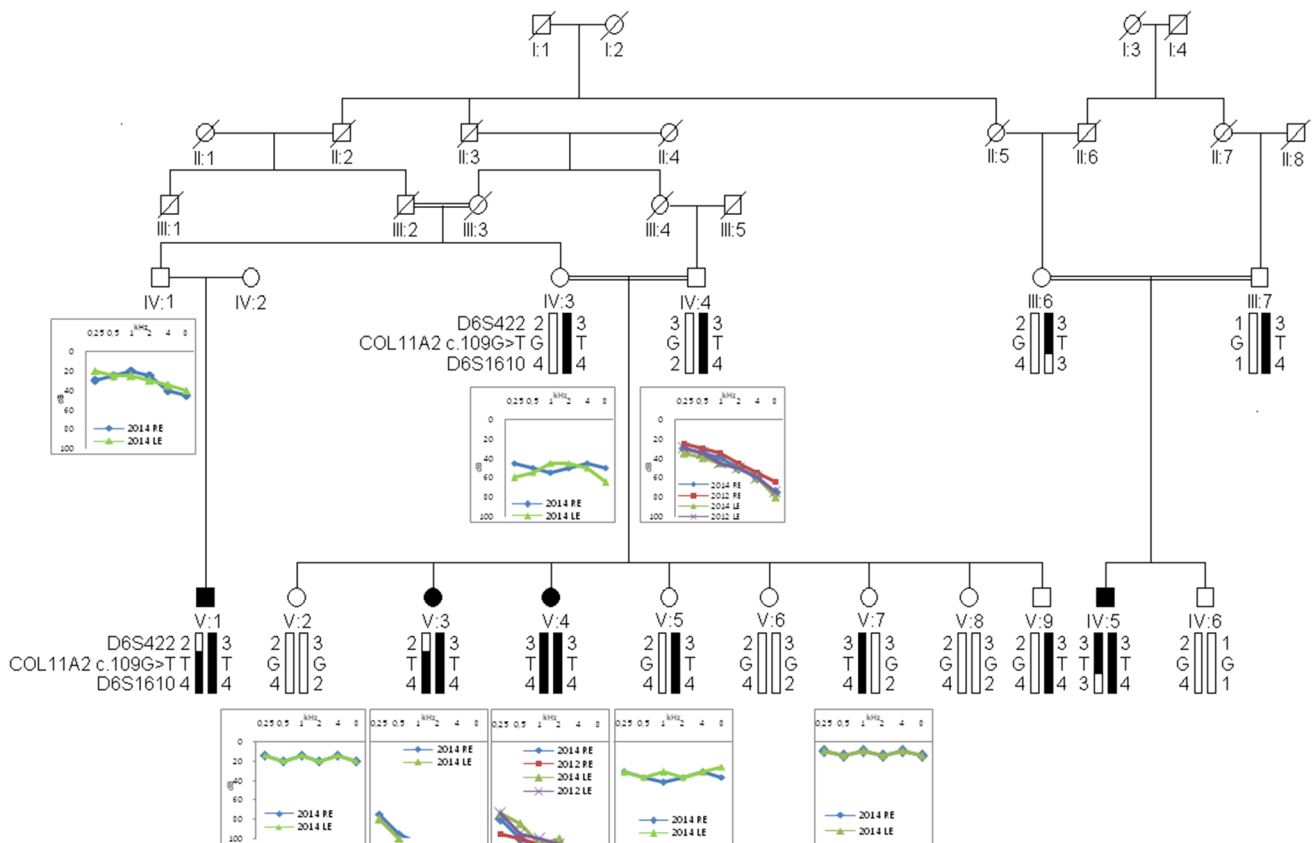
Fig. 1 Family FT3 pedigree showing audiometry data and haplotypes over the linked region on chromosome 6p21. Individuals shown in *black* have profound sensorineural hearing loss. Pure tone audiometric data obtained in 2012 and 2014 were showed for individuals

IV:1 (61 years), IV:3 (55 years), IV:4 (58 years), V:2 (34 years), V:3 (20 years), V:4 (16 years), V:5 (29 years), and V:7 (25 years). The mutation-linked haplotype is indicated by *black bar* for markers listed while other haplotypes are in *white*

Microsatellite genome-wide scan

For the family FT3 genome-wide scan was done using 400 fluorescently labeled microsatellite markers spaced in average of 10 cM/Mbp covering 22 autosomes and X chromosome (ABI PRISM® Linkage Mapping Set version 2.5 MD10, Applied Biosystems, Foster City, CA). Markers were amplified using True Allele PCR Premix and analyzed on ABI Prism 3100-Avant DNA Analyzer (Applied Biosystems, Foster City, CA).

Whole exome sequencing

Genomic DNA of one affected individual from FT3 and two affecteds from family 262 was used to sequence the whole exome as previously described (Diaz-Horta et al. 2012). Variants were filtered according to the inheritance mode (homozygous or compound heterozygous for autosomal recessive inheritance), to the function class including missense, nonsense, splice sites, in-frame indels and frameshift indels, presence and frequency at the dbSNP137 and

NHLBI (http://evs.gs.washington.edu/EVS/) databases (minor allele frequency of <0.5 % was used). We also filtered the variants for their absence in more than 2 families in our internal database that includes over 2,000 exomes, 178 of which are Turkish. For family 262, only variants that were present in both affected children were included.

Mutation analysis by sequencing genomic DNA

Variants identified in *COL11A2* have been amplified in all sampled members of Family FT3 and 262 and Sanger-sequenced on ABI models 3700 and 3100 automated sequencers (Applied Biosystems, Foster City, CA). Sequence data were aligned and compared to COL11A2 mRNA reference sequence NM_080680.2.

PCR–RFLP genotyping of missense mutation in Tunisian control individuals

Exon 2 of *COL11A2* was amplified on 40 ng genomic DNA of 113 unrelated Tunisian control individuals using forward
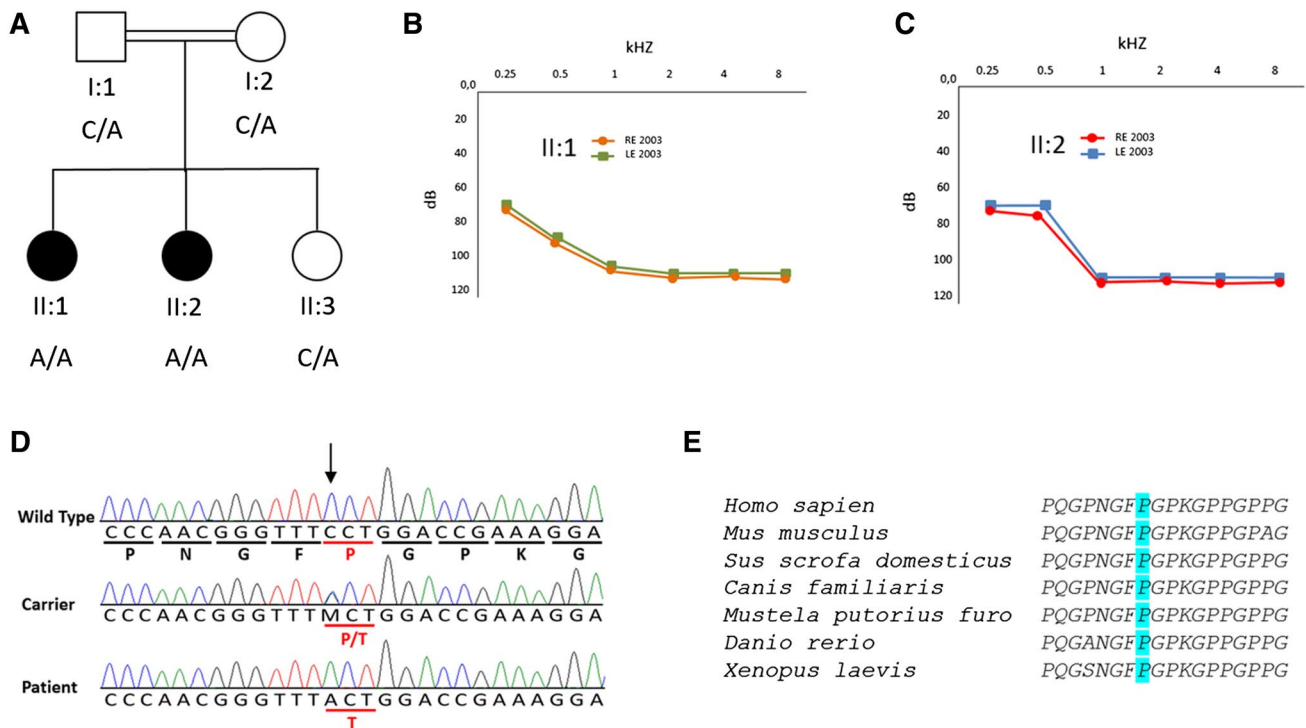
Fig. 2 Pedigree, audiogram, and mutation information of the family 262. **a** Pedigree shows two affected individuals in consanguineous family 262. **b, c** Profound bilateral hearing loss identified in both affected siblings. **d** Sanger sequencing chromatograms from deaf II:1 (Patient), parent I:1 (Carrier), and a control unrelated individual (wild type). **e** Conservation of the amino acid sequence between species around the mutation site

primer 5′-AGCAAGTGAGGGTGAGGTGAC-3′ and reverse primer 5′-TTGGGAAATCCTCCTAGTAACC-3′, then digested with ApaI restriction enzyme to yield either a 165 + 265 bp fragments (wild type allele) or 430 bp (mutant allele). DNA fragments were separated and visualized on a 2 % agarose gel.

Structural modeling of NC4 domain of COL11A2

Structural model of NC4 (also referred to as thrombospondin-like and laminin-G-like) domain (residues 23–-222) of COL11A2 was built using the MODELLER software based on homology modeling (Martí-Renom et al. 2000). Briefly, the crystal structure of NC4 domain of human COL9A1 (PDBID 2UUR) was used as a template. It should be noted that close to 50 % of residues within the putative NC4 domain of COL11A2 display strong sequence similarity, as determined by ClustalW (Larkin et al. 2007), to the canonical NC4 domain of COL9A1. A total of 100 atomic models were calculated and the structure with the lowest energy, as judged by the MODELLER Objective Function, was selected for further analysis. The structural model was rendered using RIBBONS and the electrostatic surface potential map was generated using MOLMOL (Carson 1991; Koradi et al. 1996).

GenBank accession numbers

Protein: NP_542411.2; mRNA: NM_080680.2

Results

Clinical phenotype of family FT3

The affected individuals V:1, V:3, V:4, and IV:5 of family FT3 had a history of pre-lingual HL. Pure tone audiometry showed bilateral profound sensorineural HL for affected individuals V:3 and V:4 (Fig. 1). For patient V:4, an automated auditory brainstem response (AABR) was obtained at 3 years of age and was bilaterally negative. Her parents IV:3 and IV:4 reported bilateral slowly age-related progressive HL. Pure tone audiometry showed that they had moderate sensorineural HL. The father IV:4 reported a history of professional noise exposure for 35 years. Individual V:5 had a mild HL at age 29 years. Pure tone audiometry was normal for individuals V:2 and V:7. Later, these family members were contacted for further orthopedic examination which showed no deformities. However, stature was short in all members of the family. The bone survey showed no evidence of joint degeneration, or abnormal epiphyseal

development or bone dysplasia, except for individual IV:3 whose plain radiography on lumbar spine showed a L4–L5 S1 lumbar spine degenerative disc disease, likely due to age.

The affected individuals of the Turkish originated family 262 had prelingual onset HL. Physical examination did not show short stature, disproportionate limbs, or distinct facial appearance. Pure tone audiometry showed bilateral profound sensorineural HL in both affected individuals (Fig. 2).

Identification of novel *COL11A2* mutations

Linkage analysis

DNA samples of affected individuals of the FT3 family were subjected to several molecular analyses. First, known North African mutations associated with HL had been excluded with home-built chip (Chakchouk et al. 2015). Microsatellite genome-wide scan demonstrated possible linkage with 6p21 chromosomal region. In particular, three of four affected individuals were homozygous for marker D6S1610.

Whole exome sequencing, mutation validation and analysis

We, therefore, performed WES on one affected from Family FT3 (V:4) and two affecteds from family 262 (II:1 and II:2). The exomes had on average 97, 88, and 73 % of mappable bases of the Gencode-defined exome represented by coverage of at least 2, 10, and 20 reads, respectively. Filtering of variants revealed a novel *COL11A2* mutation c.109G > T (p.Ala37Ser) in Family FT3 and another novel *COL11A2* mutation c.2662C > A (p.Pro888Thr) in Family 262. Sanger sequencing showed that both variants co-segregate with ARNSHL in families FT3 and 262 (Figs. 1, 2). Both variants were not present in the exome variant server (EVS) database (6448 exomes; http://evs.gs.washington.edu/EVS/), and dbSNP (http://www.ncbi.nlm.nih.gov/projects/SNP/) databases. Additionally 113 Tunisian healthy-hearing control individuals screened for mutation c.109G > T and the variant was absent. p.Pro888Thr was similarly absent in 178 unrelated Turkish individuals in our exome database. The COL11A2 amino acid residues Ala37 and Pro888 were highly conserved in different vertebrate and invertebrate species (Figs. 2, 3). Polyphen-2 predicted p.Ala37Ser and p.Pro888Thr as 'probably damaging' with a score of 0.967 and 1, respectively.

Molecular modeling of the novel COL11A2 mutation

To understand the molecular basis of how p.Ala37Ser mutation affects the physiological function of COL11A2,

we next modeled the structure of its N-terminal NC4 domain (residues 23–222) in homology with the known crystal structure of the NC4 domain of COL9A1 (Fig. 3c, d) (Leppanen et al. 2007). As shown in Fig. 3c, the NC4 domain of COL11A2 adopts a mixed αβ-fold with a central β-sandwich comprised of two antiparallel six-stranded β-sheets flanked between three α-helices (α1, α2 and α4) on one orthogonal face and a lone α-helix (α3) on the opposite face. Notably, the p.Ala37Ser mutation maps to α2 helix and thus could potentially cause it to unfold (Fig. 3c). The substitution of a small hydrophobic alanine with a bulkier polar serine would drastically raise the free energy of α2 helix, thereby causing it to be more stable in an unfolded conformation. This in turn will likely result in the rearrangement of neighboring helices such as α1 and α4; a scenario that could set off a domino-like effect resulting in the structural collapse of the αβ-fold of NC4 domain.

Discussion

In this study, we identified two novel *COL11A2* mutations to cause ARNSHL and confirm that *COL11A2* mutations are the cause of DFNB53. Interestingly, in family FT3, carriers of the p.Ala37Ser mutation had apparently progressive sensorineural HL after age 30 years. This observation is similar to those reported in carriers of *GJB2* 167delT and 35delG mutations who had normal hearing but were found to have subtle differences in their otoacoustic emissions, suggesting that the expression of mutations in *GJB2* may be semi-dominant (Morell et al. 1998).

Collagen XI molecules are heterotrimers of three distinct subunits, α 1(XI), α 2(XI), and α 3(II), encoded by *COL11A1, COL11A2,* and *COL2A1,* respectively (Wu and Eyre 1995). The first two subunits are closely related to α-1(V), suggesting that various combinations of these polypeptides may assemble to produce the triple helical structure of type XI collagen or heterotypic V/XI molecules (Kimura et al. 1989; Zhidkova et al. 1995; Vuoristo et al. 1996). Mice with a targeted disruption of *Col11a2* have moderate-to-severe hearing impairment in association with altered architecture of the tectorial membrane (McGuirt et al. 1999). Phenotype–genotype comparisons for *COL11A2* mutations suggest that the different phenotypes are mutation type dependent. Nonsense and frameshift mutations cause the very severe phenotypic effects associated with *COL11A2* gene such as OSMED syndrome (Tokgöz-Yılmaz et al. 2011). However, missense mutations are responsible, in general, for non-syndromic disease, in particular deafness (Fig. 4). Thirteen out of 15 missense mutations are located in the triple helical region of COL11A2. The common feature of this region is the sequential
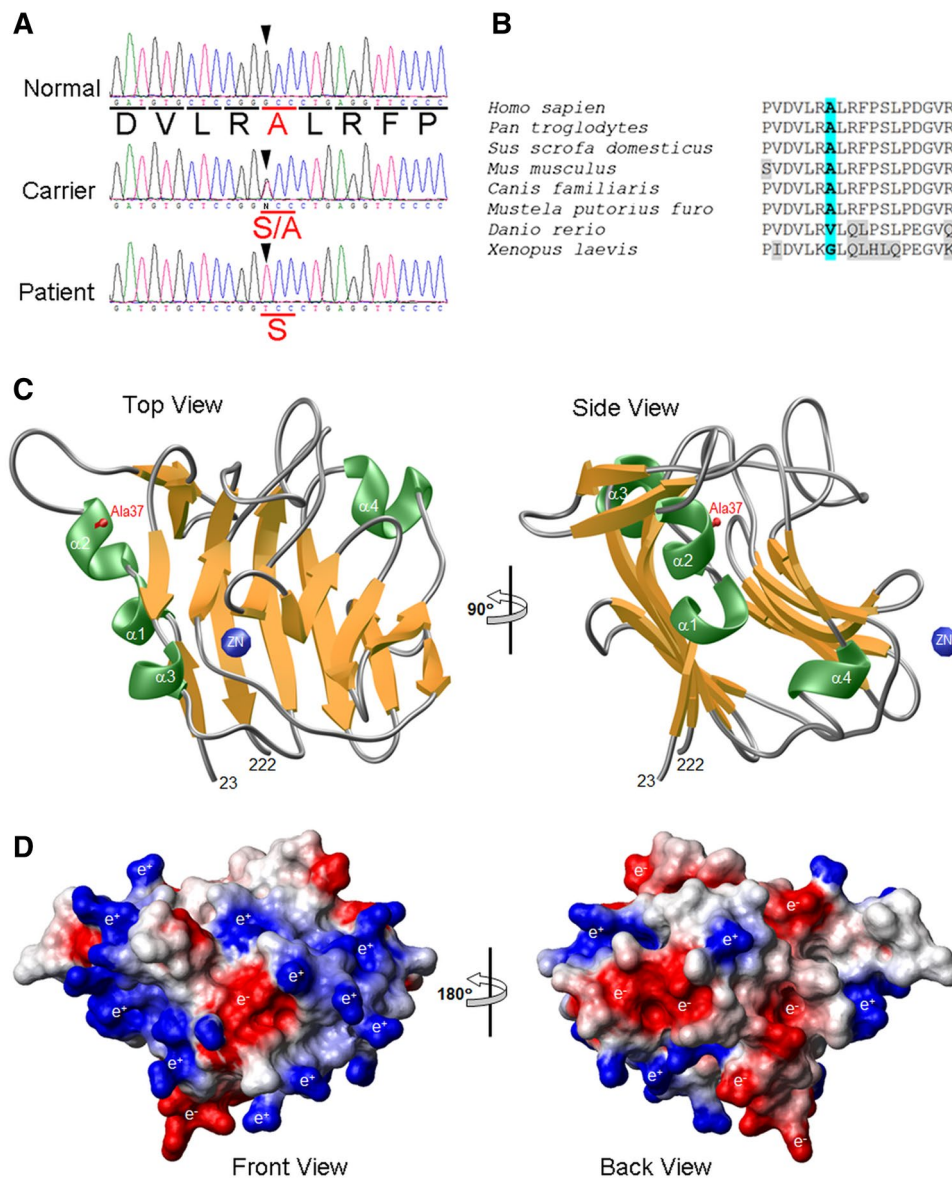
Fig. 3 Identification of c.109G > T mutation in family FT, and structural analysis of its consequence on COL11A2 biochemical properties. **a** Sequence chromatograms from deaf V:4 (Patient), parent IV:4 (Carrier), and a control unrelated individual (Normal). **b** Amino acid sequence conservation between species in and around the mutation site. **c** Ribbon representation of the structural model of NC4 domain (residues 23–222). For the inquisitive eye, two alternative orientations of NC4 domain related by 90°-counterclockwise rotation about the vertical axis are displayed. Within each orientation, the NC4 domain is color-coded with the α-helices, β-strands, and the intervening loops, respectively, shown in *green*, *yellow*, and *gray*. Additionally, the sidechain atoms of Ala37 are colored red and the Zn^{2+} divalent ion, coordinated to the NC4 domain via tetrahedral geometry, is shown as *blue* sphere. The numerals 23 and 222, respectively, indicate the N-terminal and C-terminal residue boundaries of the modeled NC4 domain within the full-length COL11A2. **d** Electrostatic surface potential map of NC4 domain. Two alternative orientations of surface charge distribution, related by 180°-counterclockwise rotation about the *vertical axis*, are shown for closer examination. Within each orientation, the *blue* and *red* colors, respectively, denote the density of positive (e+) and negative (e−) charges, while the apolar and polar surfaces are represented by *white/gray* color on the molecular surface. Note that the NC4 domain displays electrostatic polarization with one face (*Front View*) of the molecule predominantly harboring a net positive charge while the opposite face (*Back View*) carries a slightly net negative charge (color figure online)

repetition of the amino acid triplet -Gly-X–Y-, in which many of the X- and Y- positions are filled by the ring amino acids proline and hydroxyproline, required to form and stabilize the triple helix. It is noteworthy that

nine missense mutations affect glycine or proline amino acids (Fig. 4). In the Tunisian family, the novel missense mutation p.Ala37Ser is located in the N-terminus of the COL11A2 protein. The mutation does not affect
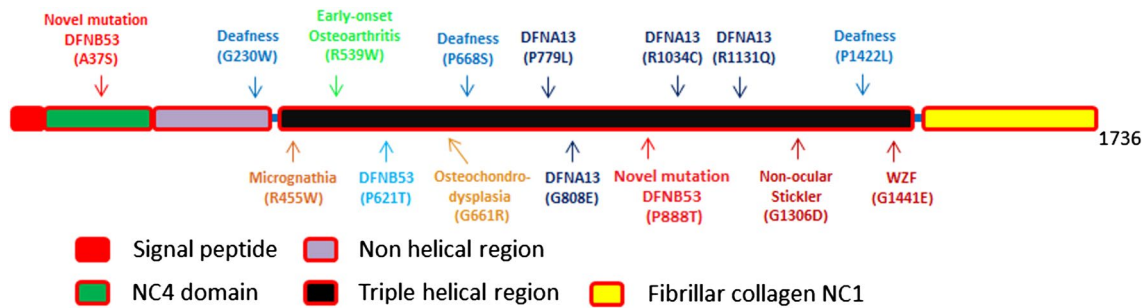
Fig. 4 A summary of novel and reported (The Human Gene Mutation Database (HGMD®, http://www.hgmd.cf.ac.uk/ac/index.php) missense mutations in collagen 2(XI) chain precursor

the -Gly-X–Y- triplet repeat motif and is located in the NC4 domain of the protein. NC4 structural architecture of COL11A2 is shared by a large number of lectin-like, thrombospondin-like, and laminin-G-like domains (Murzin et al. 1995; Lo Conte et al. 2000). Together, this superfamily of protein conducts a myriad of cellular functions by virtue of their ability to recruit a wide variety of negatively charged sulfated glycans such as heparins as well as steroids and other cellular proteins. The NC4 domain of the related COL9A1 has indeed been shown to bind to heparin in vitro (Pihlajamaa et al. 2004; Leppanen et al. 2007). Consistent with this observation, the surface potential view of NC4 domain of COL11A2 reveals that it is electrostatically polarized in that one face of the molecule predominantly harbors a net positive charge while the opposite face carries a slightly net negative charge (Fig. 3d). Such disproportionate charge distribution combined with a pKa value of close to 10 is strongly indicative of the fact that the NC4 domain of COL11A2 most likely interacts with polyanionic glycans such as glycosaminoglycans (uronic acid and keratan sulfate). In this context, our structural model suggests that the p.Ala37Ser mutation will likely obliterate, or at least partially compromise, the ability of NC4 domain to interact with its cognate ligands.

In summary, here we report clinical, genetic, and molecular characteristics of two families with DFNB53. Previously there was only one family reported with DFNB53 with a mutation in *COL11A2*. We thus confirm that *COL11A2* mutations are the cause of DFNB53. All homozygous individuals in both families had early onset profound hearing loss across all frequencies. Interestingly, in one family, aging parents who were heterozygous for the p.Ala37Ser mutation showed signs of accelerated age-related HL. The identification of additional disease-causing mutations in DFNB53 further confirms the crucial role of the COL11A2 protein in auditory function and may also shed new light on genotype–phenotype correlation and clinical follow-up of *COL11A2* mutations.

References

Carson M (1991) Ribbons 2.0. J Appl Crystallogr 24:958–961

Chakchouk I, Ben Said M, Jbeli F et al (2015) NADf chip, a two-color microarray for simultaneous screening of multigene mutations associated with hearing impairment in North African Mediterranean countries. J Mol Diagn. doi:10.1016/j.jmoldx.2014.11.003

Chen W, Kahrizi K, Meyer NC et al (2005) Mutation of *COL11A2* causes autosomal recessive non-syndromic hearing loss at the DFNB53 locus. J Med Genet 42:e61

Diaz-Horta O, Duman D, Foster J et al (2012) Whole-exome sequencing efficiently detects rare mutations in autosomal recessive non-syndromic hearing loss. PLoS ONE 7:e50628

Kimura T, Cheah KS, Chan SD et al (1989) The human α2(XI) collagen (COL11A2) chain. Molecular cloning of cDNA and genomic DNA reveals characteristics of a fibrillar collagen with differences in genomic organization. J Biol Chem 264:13910–13916

Koradi R, Billeter M, Wuthrich K (1996) MOLMOL: a program for display and analysis of macromolecular structures. J Mol Graph 14:51–55

Larkin MA, Blackshields G, Brown NP et al (2007) Clustal W and Clustal X version 2.0. Bioinformatics 23:2947–2948

Leppanen VM, Tossavainen H, Permi P et al (2007) Crystal structure of the N-terminal NC4 domain of collagen IX, a zinc binding member of the laminin–neurexin-sex hormone binding globulin (LNS) domain family. J Biol Chem 282:23219–23230

Lo Conte L, Ailey B, Hubbard TJ et al (2000) SCOP: a structural classification of proteins database. Nucleic Acids Res 28:257–259

Martí-Renom MA, Stuart AC, Fiser A et al (2000) Comparative protein structure modeling of genes and genomes. Annu Rev Biophys Biomol Struct 29:291–325

McGuirt WT, Prasad SD, Griffith AJ et al (1999) Mutations in *COL11A2* cause non-syndromic hearing loss (DFNA13). Nat Genet 23:413–419

Morell RJ, Kim HJ, Hood LJ et al (1998) Mutations in the connexin 26 gene (GJB2) among Ashkenazi Jews with nonsyndromic recessive deafness. N Engl J Med 339:1500–1505

Murzin AG, Brenner SE, Hubbard T, Chothia CA (1995) Structural classification of protein database for the investigation of sequences and structures. J Mol Biol 247:536–540

Pihlajamaa T, Lankinen H, Ylostalo J et al (2004) Characterization of recombinant amino-terminal NC4 domain of human collagen IX: interaction with glycosaminoglycans and cartilage oligomeric matrix protein. J Biol Chem 279:24265–24273

Tokgöz-Yılmaz S, Sahlı S, Fitoz S et al (2011) Audiological findings in otospondylomegaepiphyseal dysplasia (OSMED) associated with a novel mutation in COL11A2. Int J Pediatr Otorhinolaryngol 75:433–437

Vuoristo MM, Pihlajamaa T, Vandenberg P et al (1996) Complete structure of the human COL11A2 gene: the exon sizes and other features indicate the gene has not evolved with genes for other fibriller collagens. Ann NY Acad Sci 785:343–344

Wu JJ, Eyre DR (1995) Structural analysis of cross-linking domains in cartilage type XI collagen. Insights on polymeric assembly. J Biol Chem 270:18865–18870

Yan D, Tekin M, Blanton SH, Liu XZ (2013) Next-generation sequencing in genetic hearing loss. Genet Test Mol Bioma 17:581–587

Zhidkova NI, Justice SK, Mayne R (1995) Alternative mRNA processing occurs in the variable region of the pro-alpha 1(XI) and pro-alpha 2(XI) collagen chains. J Biol Chem 270:9486–9493